ICARUS **126,** 293–300 (1997)
ARTICLE NO. IS965652

A Note on the Solar Radiation Perturbations of Lunar Motion

DAVID VOKROUHLICKÝ

Institute of Astronomy, Charles University, Švédská 8, 15000 Prague, Czech Republic
E-mail: vokrouhl@beba.cesnet.cz

Received July 5, 1996; revised November 19, 1996

Solar-radiation and thermal-force effects acting on the Earth and the Moon are studied in detail. Their essential contribution to the lunar geocentric motion consists of a synodic "in-phase" oscillation with 3.65 ± 0.08 (realistic error) millimeters amplitude. This correction must be taken into account when searching for a hypothesized equivalence principle violation signal in the lunar laser ranging data.

1. INTRODUCTION

Thanks to the very high quality lunar laser ranging (LLR) data the Moon's motion is a superb testing ground for gravitation theory, including its first post-Newtonian (1PN) order relativistic structure. Testing different versions of the equivalence principle hypothesis, measuring the de Sitter precession, and searching for a secular variation of the gravitational "constant" (Dickey *et al.* 1994, Williams *et al.* 1996) have been the chief goals of LLR data analysis. An extension toward searches for more speculative 1PN effects has been recently revisited (Nordtvedt 1994, 1995, Damour and Vokrouhlický 1996b, Müller *et al.* 1996).

The estimation procedure of any parameter suffers whenever unmodeled effects of other origins produce similar range signals. For example, the secular changes which will be produced in the lunar orbit from a changing gravitational coupling parameter—"$\dot{G}/G$"—are indistinguishable over a short time span at leading order from perturbations caused by the tidal interaction between Earth (solids and oceans) and the Moon. Such problems can be avoided if the masking effects can be calculated and eliminated from or accounted for in the range data. This paper considers a similar effect needing modeling in the range signal of synodic month period.

A signal of equivalence principle violation, if present, is mostly an oscillation of synodic frequency (Nordtvedt 1995, Damour and Vokrouhlický 1996a), with only minor sidebands due to the lunar orbit's eccentricity and solar tidal distortions (Nordtvedt 1996). It is thus of high importance to "clean" this synodic frequency from other unmodeled effects. A most recent numerical fit of the lunar orbit by Williams *et al.* (1996) finds a -1.2 ± 1.3-cm "realistic" uncertainty unexplained synodic signal amplitude, the best-fit value of -1.2 cm being statistically significant at a very high level. The effects studied in this paper explain part of this amplitude and reduce the remainder.

Nordtvedt (1995) has pointed out that the radiation-related effects on the Moon and Earth are important synodic perturbations not yet included in the LLR model (see also Williams *et al.* 1996), and he estimated that they contribute a few millimeters to the synodic amplitude.[1] This has motivated us to examine in detail the problem of radiative and thermal perturbations of the lunar motion. To our knowledge, it is the first case in which motion of a major Solar System body needs consideration of radiation pressure forces.

The characteristic size of the lunar acceleration due to solar radiation pressure is obtained from the total radiation momentum intercepted by the Moon per unit time,

$$A_{\rm rad} = \Phi_0 \frac{\pi R^2}{Mc}, \tag{1}$$

where Φ_0 is the solar constant, R the lunar radius, M its mass, and c light velocity. This acceleration mimics an equivalence-principle-violating relative acceleration, and (1) can be simply converted into a characteristic synodic amplitude of oscillation (Nordtvedt 1995, Damour and Vokrouhlický 1996a),

$$|\delta r|_{\rm syn} = \frac{3}{2} \frac{S(m)}{n'(n-n')} A_{\rm rad}, \tag{2}$$

in which $m = n'/(n - n')$ is the Hill parameter [$m \simeq 0.08085$ for the Moon], and the amplification function $S(m)$ results from the coupling of the solar radiation pressure perturbation with the solar quadrupole tide deformation of

[1] Actually, the quoted effects affect all principal relativistic tests listed above, but in this paper we focus on aliasing with the free-fall hypothesis test.

0019-1035/97 $25.00

the lunar orbit [$S(m) \simeq 1.622$ for the Moon; see Nordtvedt (1995) and Damour and Vokrouhlický (1996a)]. Substituting numerical factors into (2), one obtains $|\delta r| = 2.95$ mm.

To include a more general model of radiation effects (variable reflectance patterns on the lunar surface, radiation pressure exerted on the Earth, thermal effects, etc.), Nordtvedt (1995) assumed the net nongravitational acceleration **a** of the Moon relative to Earth can be given by

$$\mathbf{a}/A_{\rm rad} = -\{[1 + f(\tau)]\hat{\mathbf{R}} + f'(\tau)\hat{\mathbf{T}}\}, \tag{3}$$

with the functions $f(\tau)$ and $f'(\tau)$ developable in Fourier series,

$$f(\tau) = \bar{f} + f_{\rm c}\cos\tau + f_{\rm s}\sin\tau + f_{2\rm c}\cos 2\tau + f_{2\rm s}\sin 2\tau + \ldots, \tag{4}$$

$$f'(\tau) = \bar{f}' + f'_{\rm c}\cos\tau + f'_{\rm s}\sin\tau + f'_{2\rm c}\cos 2\tau + f'_{2\rm s}\sin 2\tau + \ldots. \tag{5}$$

Here, τ is the Sun–Moon phase angle, $\hat{\mathbf{R}}$ is a unit position vector toward the Sun, and $\hat{\mathbf{T}}$ is a unit normal to $\hat{\mathbf{R}}$ in the plane of ecliptic and pointing in sense of increasing τ. Because the Moon is locked in 1:1 spin-orbit motion, the lunar phase angle τ also indicates its approximate rotation phase.[2]

Each of the coefficients ($\bar{f}, \bar{f}', f_{\rm c}, f'_{\rm c}, \ldots$) corresponds to lunar orbit perturbation with characteristic frequency, and can be submitted to the general perturbation-theory scheme (see Nordtvedt (1995), for a recent review of analytical techniques of the lunar relativistic perturbations see Nordtvedt and Vokrouhlický (1997)). Nordtvedt (1995) developed the first steps in this analysis and showed that of primary interest are the coefficients $\bar{f}$ and $\bar{f}'$. In this paper, we estimate, by using detailed numerical models, values of these two coefficients (we call $\bar{f}$ the "in-phase" parameter and $\bar{f}'$ the "out-of-phase" parameter, owing to the phase of their dynamical effect on the lunar orbit; see Nordtvedt (1995)). Our results indicate that the characteristic synodic amplitude (2) from radiation absorption is increased by about 25%, being the net result of the additional force on the Moon from its radiant reemissions, and of the similar absorption and reemission by the Earth. The estimated total amplitude of synodic oscillation of lunar motion due to all radiation effects is 3.65 mm. An important part of our study consists of careful estimation of the error of the above-mentioned results due to insufficient and/or bad modeling of radiative effects. Our tests indicate 2% as a realistic value of the above-mentioned error. Part of this error is also due to the tiny contribution of the unestimated second-order coefficients $f_{2\rm c}$, $f_{2\rm s}$, $f'_{2\rm c}$, and $f'_{2\rm s}$ to the synodic perturbation of the lunar orbit (Nordtvedt 1995).

[2] The mean inclination of the lunar axis to the ecliptic does not exceed 1.6°, so we shall assume throughout this paper that the Moon's spin is normal to the ecliptic.

2. RADIATION FORCES

Solar radiation absorbed and reflected on Earth and Moon surfaces exerts force on the two bodies. An estimate of the force per unit of mass (acceleration) related to the absorbed radiation by the Moon is given by Eq. (1). Coefficients $\bar{f}$ and $\bar{f}'$ express acceleration of the Moon due the additional physical causes of the radiative/thermal origin as a fraction of the lunar acceleration due to directly absorbed sunlight. As they can be separated into contribution of several effects we shall label each individual contribution by an appropriate index. They can be listed as follows:

1. $\bar{f}_{\rm E}$, resp. $\bar{f}'_{\rm E}$, terms given by radiation acceleration of the Earth due to absorbed sunlight;
2. $\bar{f}_{A_{\rm E}}$, resp. $\bar{f}'_{A_{\rm E}}$, terms given by radiation acceleration of the Earth due to reflected and/or scattered sunlight on its surface and/or atmosphere;
3. $\bar{f}_{A_{\rm M}}$, resp. $\bar{f}'_{A_{\rm M}}$, same as in 2, but for the Moon;
4. $\bar{f}_{\rm TH}$, resp. $\bar{f}'_{\rm TH}$, terms given by the thermal acceleration of the Moon.

Each of these coefficients is discussed in some detail below.

As it is most convenient to investigate the lunar motion in the geocentric reference frame, one must subtract the radiation induced acceleration of the Earth from the total perturbing effect acting on the lunar motion. As concerns the absorbed sunlight by the Earth we can use formula (1) provided that the Earth parameters (M' for mass and R' for radius) are considered. The corresponding piece of the $\bar{f}$-factor reads

$$\bar{f}_{\rm E} = -\frac{M}{M'}\left(\frac{R'}{R}\right)^2. \tag{6}$$

Numerically, one gets $\bar{f}_{\rm E} = -0.167$. Obviously, $\bar{f}'_{\rm E} = 0$.

The intricate part of the radiation acceleration is related to the sunlight reflected on the two bodies (or scattered in the Earth's atmosphere; items 2 and 3 in the above list). Their first estimate is given by assuming diffuse (Lambertian) reflection on the two bodies with average plane albedo values $\overline{A}_{\rm M}$ (Moon) and $\overline{A}_{\rm E}$ (Earth). Then, approximately, we have

$$\bar{f}_{A_{\rm M}} \simeq \frac{4}{9}\overline{A}_{\rm M}, \tag{7}$$

$$\bar{f}_{A_{\rm E}} \simeq -\frac{4}{9}\overline{A}_{\rm E}\,\frac{M}{M'}\left(\frac{R'}{R}\right)^2. \tag{8}$$

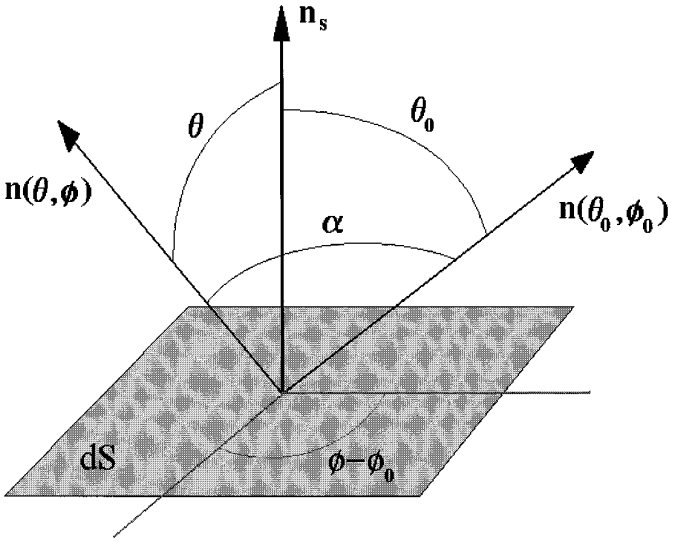

FIG. 1. Angular parameters characterizing reflection of sunlight on a local (Earth's or Moon's) surface element dS. The spherical angles (θ, ϕ) correspond to the reflected light ray, while (θ_0, ϕ_0) correspond to the incident sunlight. Angle α between the two directions.

Substituting the average values of the plane albedo for the two bodies ($\overline{A}_{\rm M} \simeq 0.08$ and $\overline{A}_{\rm E} \simeq 0.3$), we obtain $\bar{f}_{A_{\rm M}} \simeq 0.036$ and $\bar{f}_{A_{\rm E}} \simeq -0.022$, i.e., about a 1% total effect. In the rest of this section, we try to substantiate the validity of such simple estimates by introducing more detailed models of sunlight reflection for both bodies.

We approximate the solar radiation in the Earth and Moon vicinity by a simple homogeneous force field. However, for further use we need sufficiently general tools for description of the radiation field of the sunlight reflected on the Earth or Moon surfaces (and also the lunar thermal field). We shall speak in terms of the radiative intensity (or "brightness") I, which physically denotes the amount of radiation energy emitted by unit surface element into a unit solid angle per unit of time (for definition see, for instance, Mihalas (1978)). Introducing a local coordinate system attached to the given surface element with its z-axis coinciding with surface normal $\mathbf{n}_S$, and introducing spherical coordinates (θ, ϕ) in this system, we write a sufficiently general reflection law in the form

$$I(\mu, \mu_0; \alpha) = \frac{\Phi_0}{\pi} \mu_0 R(\mu, \mu_0; \alpha), \tag{9}$$

where $\mu = \cos\theta$, "0" indicates quantities for local solar position, and

$$\cos\alpha = \mu\mu_0 + \sqrt{(1-\mu^2)(1-\mu_0^2)}\cos(\phi - \phi_0). \tag{10}$$

Figure 1 shows angular parameters introduced above. Notice, that the spherical angle θ is measured from the local normal $\mathbf{n}_{\rm S}$, and origin of the angle ϕ is irrelevant because the brightness (9) of the reflected radiation depends only on a difference $(\phi - \phi_0)$. The function $R(\mu, \mu_0; \alpha)$ in (9) includes directional characteristics of the reflection. The simplest case, already mentioned above $R_{\rm L}(\mu, \mu_0; \alpha) = A$, is called Lambertian (or diffuse) reflection with a plane albedo A. Such a type of reflection/emission law holds well for thermal (long-wave) emission, but typically it fails to represent reflection of the visible light both on Earth's and the Moon's surfaces. We shall give more complicated reflection functions $R(\mu, \mu_0; \alpha)$ in appropriate sections below.

On fixing the reflection law $R(\mu, \mu_0; \alpha)$, we may compute the radiation force acting on a unit surface element by

$$\mathbf{f} = \frac{\Phi_0}{\pi c} \mu_0 \int_\Omega d\Omega\, \mu R(\mu, \mu_0; \alpha)\mathbf{n}(\mu, \phi), \tag{11}$$

where the integration domain Ω represents the whole half-space above the surface element, and $d\Omega = d\mu d\phi$. Related acceleration per unit of surface is expressed as force (11) divided by corresponding mass. For the case of the Lambertian reflection/emission we can evaluate (11) analytically with the following result:

$$\mathbf{f}_{\rm L} = \frac{2}{3}\frac{\Phi_0}{c} A\mu_0 \mathbf{n}_{\rm S}. \tag{12}$$

Integrating (12) over the illuminated hemisphere of a spherical body directly yields formula (7) for the corresponding force $\bar{f}$-factor.

2.1. Lunar Radiation Acceleration

Individual optical patterns are distributed inhomogeneously on the lunar surface, which, together with slow lunar rotation, results in nonvanishing coefficients ($f_{\rm c}, f_{\rm s}, f'_{\rm c}, f'_{\rm s}, \ldots$) in the developments (4) and (5). However, as we concentrate on a precise estimation of the mean values $\bar{f}_{A_{\rm M}}$ and $\bar{f}'_{A_{\rm M}}$, we use averaged models of the lunar reflection, neglecting individual local anomalies.

The fact that lunar surface reflection of the solar radiation significantly deviates from the Lambert law has been conjectured for a long time (e.g., Fessenkov 1962). This finding has been confirmed by the first modern work on this topic by Pettit and Nicholson (1930). Since then, many precise data have been accumulated and diverse methods suggested for their interpretation. We decided to use the approach of Lumme and Bowell (1981). They developed a precise model of sunlight reflection on the porous and rough lunar surface, and they showed that the general formulae can be with sufficient precision approximated by

$$R(\mu,\mu_0;\alpha)=\frac{1}{4}\frac{\omega_0}{\mu+\mu_0}\left[2\frac{1-g^2}{(1+g^2+2g\cos\alpha)^{3/2}}\frac{\Phi_S(\alpha)}{1+\rho\xi}+h(\mu)h(\mu_0)-1\right], \quad (13)$$

with

$$\xi=\sqrt{\mu^2+\mu_0^2-2\mu\mu_0\cos\alpha}/(\mu\mu_0), \quad (14)$$

$$\Phi_S(\alpha)=\exp\left[-\frac{\sin\alpha}{0.636D+1.828\sin\alpha}\right], \quad (15)$$

$$h(\mu)=1+a_1\mu+a_2\mu^2, \quad (16)$$

where coefficients a_1 and a_2 are functions of the fundamental parameters; ω_0, a single scattering albedo; and g, Henyey–Greenstein asymmetry factor (see Lumme and Irvine 1982). Lumme and Irvine (1982) used an extensive set of lunar photometry data for estimating best values of the theory parameters and obtained $\omega_0 = 0.42 \pm 0.05$ and $g = -0.094 \pm 0.043$ in the visible band (assuming $D = 0.37$ for the volume density of the lunar surface layer and $\rho = 0.86$ for the "roughness parameter"). The negative value of g-factor corresponds to backscattering properties of lunar soil (resulting in "the opposition effect"; Lumme and Bowell (1981)). To visualize this phenomenon, we plot in Fig. 2 reflectance profile $\mu_0 R(\mu,\mu_0;\alpha)$ in the solar plane ($\phi - \phi_0 = 0$ and π) for several sunlight incidence angles. We note a strong backscatter of the solar radiation for large incidence angles θ_0.

Introducing auxiliary functions

$$\psi(\mu_0)=\mu_0\int_0^\pi d\phi\int_0^1 d\mu\,\mu^2 R(\mu,\mu_0;\alpha), \quad (17)$$

$$\psi'(\mu_0)=\mu_0\int_0^\pi d\phi\cos\phi\int_0^1 d\mu\,\mu\sqrt{1-\mu^2}R(\mu,\mu_0;\alpha), \quad (18)$$

we express the searched $\bar{f}$ value related to sunlight reflection on the Moon's surface by

$$\bar{f}_{A_M}^{(LI)}=\frac{4}{\pi}\int_0^1 d\mu_0\left[\mu_0\psi(\mu_0)+\sqrt{1-\mu_0^2}\psi'(\mu_0)\right] \quad (19)$$

(and $\bar{f}'_{A_M} = 0$). We integrated numerically (19) with Lumme–Irvine lunar fitted values of ω_0 and g parameters and obtained $\bar{f}_{A_M}^{(LI)} = 0.041 \pm 0.006$, a value slightly greater than the 0.036 estimated in (7) from the diffuse approximation with averaged lunar plane albedo $\overline{A}_M \simeq 0.08$. The difference between the two values can be attributed to lunar soil backscattering, which clearly tends to amplify the radiation pressure. However, the entire gain is not significant.

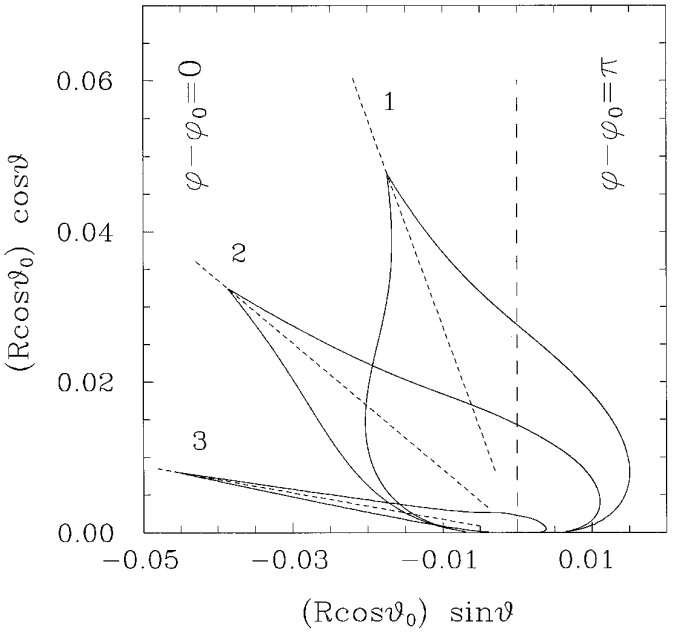

FIG. 2. Indicatrix of the Lumme–Irvine reflection model on lunar regolith in the Sun-normal plane $\phi - \phi_0 = 0$ and π [polar coordinate plot with "angle" measured from the solar direction given by a short-dashed line and "radius" given by reduced intensity $\mu_0 R(\mu,\mu_0;\alpha)$]. Three incidence angles of the sunlight were chosen: (a) $\theta_0 = 20°$, curve 1; (b) $\theta_0 = 50°$, curve 2; (c) $\theta_0 = 80°$, curve 3. Long-dashed line shows normal to the lunar surface. The backscatter properties are significant for large sunlight incidence angles (case 3).

2.2. Radiation Acceleration of the Earth

The perturbing effect of the direct solar radiation pressure on the Earth has been already discussed in Section 2 [Eq. (6)]. Hereinafter, we consider effects related to sunlight reflected on the Earth surface and/or scattered in the Earth atmosphere. In accordance with notation in Section 2 we shall denote the corresponding force factors $\bar{f}_{A_E}$ and $\bar{f}'_{A_E}$. Because three different models of the Earth's surface nature are considered below, we label the corresponding factors with superindeces (1) to (3).

In the first test, we shall neglect atmospheric effects (clouds) and the special nature of the ocean-surface reflection, taking into account only the seasonally averaged Earth albedo distribution model. We adopted the model of Sehnal (1979) which yields colatitude (ϑ') and longitude (φ') dependent Earth albedo $A_E(\vartheta',\varphi')$ in terms of spherical harmonic development (qualitatively, we checked that the results of the Sehnal model match those of similar models; e.g., Stephens *et al.* (1981)). Employing (12) we find the following expression for the "in-phase" coefficient

$$\bar{f}_{A_E}^{(1)}=-\frac{2}{3\pi}\int_{\Omega'}d\Omega'\cos^2\vartheta' A_E(\vartheta',\varphi') \quad (20)$$

$[d\Omega' = d(\cos\vartheta')\,d\varphi']$. The corresponding contribution to the "out-of-phase" factor $\bar{f}'$ is very small and will be neglected here. Integration domain Ω' in (20) is given by the illuminated part of the Earth surface and thus depends on the solar position. We performed 10^4 test computations of (20) with randomly chosen solar position, and obtained $\bar{f}^{(1)}_{A_E} = -0.018 \pm 0.004$. This value is a bit smaller than our previous rough estimate (8), because the Earth equatorial regions have albedo values smaller than the average $\overline{A}_E$ and the Sun lies preferentially in the near-equatorial regions.

In the following, we show that there are two refinements which act oppositely in changing $\bar{f}_{A_E}$: (i) reflection of sunlight on the ocean surfaces, which tends to increase $\bar{f}^{(1)}_{A_E}$, because of low ocean albedo and specular-like scattering, and (ii) scattering of sunlight in clouds, which tends to decrease the previously estimated value of $\bar{f}^{(1)}_{A_E}$ due to higher cloud albedo. Thanks to satellite Earth-photometry missions, there exists a large sample of data on properties of sunlight reflection on diverse Earth-surface structures (land, oceans, polar regions, clouds, etc.). We shall employ results of NIMBUS 7 experiment broadly investigated in the literature (e.g., Taylor and Stowe 1984; Rubincam *et al.* 1987, Mokhov and Schlesinger 1994).

Reflection of solar radiation on the ocean surfaces and polar ice-covered regions shows a strong forward, specular-like scattering (see Taylor and Stowe 1984), especially for large incidence angles of the solar radiation. Rubincam *et al.* (1987) fitted the satellite born data of Taylor and Stowe (1984) and obtained a simple representation of the directional ocean reflectance

$$R_{oc}(\mu, \mu_0; \alpha) = (0.45 - 0.35\mu_0)[c_1 \exp(-\psi/\psi_0) + 0.6 \exp(3\mu/\pi)]/B, \quad (21)$$

with $\cos\psi = 2\mu\mu_0 - \cos\alpha$, $c_1 = 6 - 5.3\mu_0$, and $\psi_0 = (\pi/9)(1 + \mu_0)$. Denominator term B is determined by normalization of $R(\mu, \mu_0; \alpha)$ to unity. The first term in the bidirectional function (21) models specular-like patterns of reflection, while the second corresponds to the observed limb brightening. Again, we performed 10^4 test runs, locating the Sun randomly on the ecliptic, and computed $\bar{f}$ "in-phase" factor with the Rubincam *et al.* directional function (21). In our calculation we used a detailed ocean mask on the Earth surface, deciding individually whether the Earth surface element contributing to the total force-factor belongs to continent or ocean. Our final result, $\bar{f}^{(2)}_{A_E} = -0.013 \pm 0.003$, is approximately by a factor 1.5 smaller than $\bar{f}^{(1)}_{A_E}$. There are two principal reasons: (i) the ocean albedo is significantly smaller than that of continents (Taylor and Stowe 1984), and (ii) forward (specular-like) scattering of sunlight does not contribute to the total force exerted on the Earth's illuminated hemisphere.

The plane albedo of clouds depends on the sunlight incidence angle, growing to 0.75 for nearly surface-grazing illumination (see Fig. 9 in Taylor and Stowe 1984). Similarly to the ocean surface and icy-region reflection, forward scattering with the mean Henyey–Greenstein asymmetry factor $\bar{g}_{cl} \simeq 0.85$ is observed (e.g., Fouquart *et al.* 1990). For purpose of our study, we adopted simple Chandrasekhar's model of sunlight diffusion in plane-parallel atmospheres with infinite optical thickness (Chandrasekhar 1950) and with scattering centers characterized by single-reflection albedo ω_0 and phase function $p(\chi) = \omega_0(1 + b\cos\chi)$ (χ being the scattering angle). Then, the bidirectional reflection function on top of the atmosphere reads

$$\begin{aligned} R_{cl}(\mu, \mu_0; \alpha) &= \frac{1}{4}\frac{\omega_0}{\mu + \mu_0}\{[1 - e(\mu + \mu_0) \\ &\quad - b(1 - \omega_0)\mu\mu_0]H^{(0)}(\mu)H^{(0)}(\mu_0) \\ &\quad + b\sqrt{(1 - \mu^2)(1 - \mu_0^2)}H^{(1)}(\mu)H^{(1)}(\mu_0)\cos(\phi - \phi_0)\}, \end{aligned} \quad (22)$$

where $H^{(0)}(\mu)$ and $H^{(1)}(\mu)$ are the corresponding Chandrasekhar's H functions. Their suitable approximation is given, together with moment $e(\omega_0, b)$, in Ahmad and Deering (1992). In our series of tests we chose $\omega_0 \simeq 0.92$ and $b \simeq -1$ (Irvine 1975, Fouquart *et al.* 1990). This choice fits well the observed cloud albedo dependence on solar incidence angle (θ_0): $A_{cl}(\theta_0) \simeq 0.75$–$0.15\cos\theta_0$ (e.g., Raschke *et al.* 1973, Taylor and Stowe 1984).

Obviously, we lack a predictive model for cloud distribution over the Earth surface and use statistical information only. According to satellite born data reported by Mokhov and Schlesinger (1994) the mean cloudiness is 57% with seasonal and hemispheric variations. In our third test, we randomly filled the Earth surface by clouds with this mean cloudiness occupation and integrated 10^4 configurations as before. The resulting "in-phase" force-factor is $\bar{f}^{(3)}_{A_E} = -0.031 \pm 0.004$. In comparison with $\bar{f}^{(2)}_{A_E}$ we observe a decrease due to high albedo of clouds; however, the forward scattering properties of cloud reflection increase the total computed force.

We thus conclude that (statistically) the force-factor $\bar{f}_{A_E}$ due to sunlight reflected on the Earth surface never exceeds -0.035. This limit will be taken as the "conservative" estimate of $\bar{f}_{A_E}$ in the following considerations.

3. THERMAL ACCELERATION OF THE MOON

Determination of the temperature distribution on surfaces of celestial bodies has served as an important key in several problems of Solar System physics, from determination of the surface properties to estimating asteroid radii. Occasionally, the dynamical implications of the tempera-

ture inhomogeneities have been addressed in the context of motion of the asteroids and their fragments (e.g., Peterson 1976, Burns *et al.* 1979, Rubincam 1995) and motion of artificial satellites (e.g., Rubincam 1987, Afonso *et al.* 1989, Farinella and Vokrouhlický 1996). Owing to slow rotation of the Moon, the corresponding thermal effect, studied hereafter, falls in the class of ''diurnal'' Yarkovsky effects (e.g., Peterson 1976, Burns *et al.* 1979).

Similar to the local anomalies of the sunlight reflection on the lunar surface mentioned above, there exist local thermal patterns. The thermal regime of particular craters, deep depressions, or highlands may exhibit differences from the averaged model involved below (e.g., Savail and Fanale 1994). Having in mind the proper task of this paper—estimation of the mean force factors $\bar{f}$ and $\bar{f}\,'$—it seems appropriate to avoid such local features on the lunar surface.

3.1. Thermal Model of the Lunar Soil

The heat transfer problem in the lunar soil can be approximated with sufficient accuracy by a one-dimensional diffusion equation,

$$\rho C \frac{\partial T}{\partial t} = \frac{\partial}{\partial x}\left[K(T) \frac{\partial T}{\partial x} \right], \tag{23}$$

yielding a temperature distribution $T(x, t)$ at depth x and time t. Here, we adopted the following notation: ρ, lunar surface density; C, specific heat capacity; and K, thermal conductivity of regolith. Boundary conditions which are to be considered together with (23) read

$$\varepsilon\sigma T_0^4 = K(T_0)\left(\frac{\partial T}{\partial x}\right)_0 + (1-A)F_0, \tag{24}$$

$$\left(\frac{\partial T}{\partial x}\right)_\infty = 0, \tag{25}$$

where F_0 denotes scalar radiation flux imposed on the surface, ε the infrared emissivity, σ the Stefan–Boltzmann constant, and A the plane albedo). Indexes 0 and ∞ correspond to $x = 0$ (surface) and $x \to \infty$ (''large depth''), respectively. As A ($\simeq$0.08) is very small for the lunar soil, the thermal effects turn out to be particularly important for goals of this study.

Temperature dependence of the thermal conductivity $K(T)$ is physically induced by penetration of sunlight into the porous regolith. Wesselink (1948) (followed by Glegg *et al.* 1966) derived the law

$$K(T) = K_c + K_r T^3, \tag{26}$$

with about a 52% percent contribution of the radiation diffusion term at $T \simeq 300$ K (Glegg *et al.* 1966). Introducing an averaged thermal conductivity K_0 at the reference subsolar temperature on the Moon T_{SS} [$\varepsilon\sigma T_{SS}^4 \equiv (1-A)\Phi_0$], one can estimate width of the skin layer in the lunar soil in which the thermal wave propagates by (e.g., Wesselink 1948, Spencer *et al.* 1989)

$$l_s \simeq \sqrt{\frac{K_0}{\rho n C}}. \tag{27}$$

Here, n denotes, as before, the angular synodic frequency of lunar rotation. In case of lunar soil one obtains a few-centimeter slab, which well supports the one-dimensional approximation (23). Spencer *et al.* (1989) pointed out that the solution of the thermal response of the body to the external radiative heating is uniquely determined by the value of the thermal parameter

$$\Theta = \frac{\Gamma\sqrt{n}}{\varepsilon\sigma T_{SS}^3}. \tag{28}$$

We keep Spencer *et al.* (1989) notation by denoting thermal inertia as $\Gamma \equiv \sqrt{K_0 \rho C}$. One obtains $\Gamma \simeq 50$ J m^{-2} sec$^{-1/2}$K^{-1} and $T_{SS} \simeq 392.3$ K for lunar regolith parameters, leading thus to $\Theta \simeq 0.025$. Physically, Θ expresses the ratio of the characteristic time scale for radiating the amount of accumulated energy to the rotation period of the body, i.e., ability of the surface to keep up with diurnal insolation changes (see Farinella and Vokrouhlický (1996) for further discussion).

We adopted a numerical scheme discussed in detail by Spencer *et al.* (1989) with iterative solution of the energy balance (24) on the lunar surface, a method which proved to be sufficiently fast for further use. Figure 3 shows the thermal history of surface elements at different lunar colatitudes ϑ during one lunation when the Sun is assumed to be at the lunar equator. The phase angle φ is chosen such that $\varphi = 0$ corresponds to passage of a given element through the solar meridian, so that the interval $\pi/2$ to $3\pi/2$ corresponds to ''lunar night.'' The temperature is normalized to the reference subsolar value T_{SS}. The equatorial temperature decreases down to about 100 K, in good agreement with the observations (Wesselink 1948, Sinton 1962). We notice that the temperature variations are complicated function of phase φ which cannot be easily approximated by a few first Fourier harmonics.

3.2. Lunar Thermal Acceleration

Once the temperature distribution on the lunar surface has been fixed, we can compute the corresponding thermal acceleration. The flux Φ_0 from (11) is to be expressed by the Stefan–Boltzmann law of the radiation flux of the

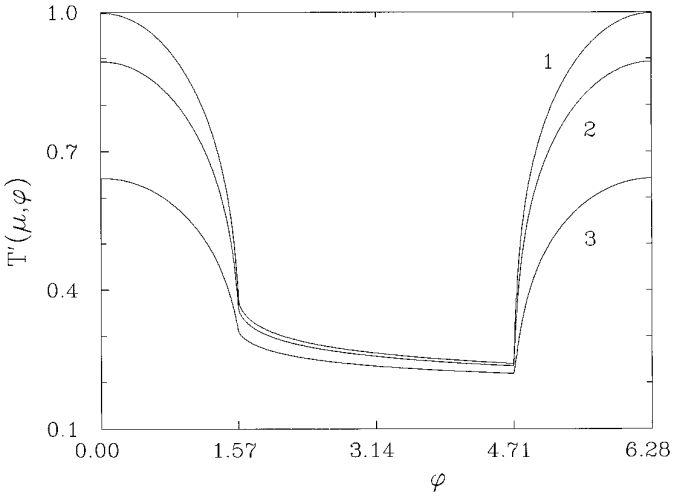

FIG. 3. Normalized temperature $T'(\mu, \varphi) = T(\mu, \varphi)/T_{SS}$ profiles during one lunar cycle (synodic month; $\mu = \cos \vartheta$). The reference subsolar temperature $T_{SS} = 392.3$ K. Three lunar colatitudes were chosen: (a) $\vartheta = 90°$, curve 1; (b) $\vartheta = 40°$, curve 2; (c) $\vartheta = 10°$, curve 3.

graybody with emissivity ε: $\varepsilon\sigma T^4$. As the temperature depends on a particular surface element on the Moon, we must integrate over the entire lunar surface S

$$\mathbf{a}/A_{\text{rad}} = -\frac{2}{3\pi}(1 - A)\int_S d\Omega(\vartheta, \varphi)T'^4(\vartheta, \varphi)\mathbf{n}(\vartheta, \varphi), \quad (29)$$

where $d\Omega = d(\cos \vartheta)\, d\varphi$ and ϑ and φ are selenographic colatitude and longitude, respectively, of a given surface element, giving the averaged factors

$$\bar{f}_{\text{TH}} = -\frac{4}{3}(1 - A)\int_0^{\pi/2+\vartheta_0} d\vartheta \sin^2 \vartheta \langle T'^4(\vartheta, \varphi) \cos \varphi\rangle, \quad (30)$$

$$\bar{f}'_{\text{TH}} = -\frac{4}{3}(1 - A)\int_0^{\pi/2+\vartheta_0} d\vartheta \sin^2 \vartheta \langle T'^4(\vartheta, \varphi) \sin \varphi\rangle, \quad (31)$$

where the angle brackets indicate that an average over longitude φ has been done. Selenographic colatitude of the Sun is denoted by ϑ_0. With the solar position on the Moon's equator ($\vartheta_0 = \pi/2$), we computed integrals (30) and (31) numerically, obtaining the following results: $\bar{f}_{\text{TH}} = 0.399$ and $\bar{f}'_{\text{TH}} \simeq 0.006$. We notice the large value of the first of the two factors, contributing to enhancement of the "in-phase" synodic oscillations of the lunar orbit.

We can compare this fully numerical result with the following very rough estimates. First, we can assume a simple law for the surface thermal wave $T' = \tau_0(1 + \tau_1 \cos \varphi)$, with $\tau_0 \simeq 0.572$ and $\tau_1 \simeq 0.748$ (e.g., Sinton 1962). Then one obtains $\bar{f}_{\text{TH}} \simeq \frac{16}{9}\tau_0^4\tau_1(1 + \frac{3}{4}\tau_1^2) \simeq 0.202$. However, thanks to very small value of the thermal parameter Θ, the standard thermal model of a nonrotating Solar System body (e.g., Lebofsky and Spencer 1989) is more appropriate to this estimate. In this case no thermal memory of the lunar soil is assumed and incident solar radiation energy is reemitted instantaneously. A simple calculation yields $\bar{f}_{\text{TH}} \simeq \frac{4}{9}(1 - \overline{A}_{\text{M}}) = 0.409$. The actual value of the in-phase parameter $\bar{f}_{\text{TH}}$ is expected to lie in between these two extreme values. Indeed, our numerical result falls in this interval and is very close to the latter estimate.

In contrast to the in-phase parameter, the "out-of-phase" factor $\bar{f}'$ is negligibly small because of small value of the lunar soil thermal parameter Θ.

Finally, we note that similar thermal effects acting on the Earth are negligible owing to combination of several circumstances: (i) fast Earth rotation, (ii) higher Earth averaged albedo, and (iii) smaller area to mass ratio. We estimated contribution of the Earth thermal effects for the computed $\bar{f}$ factors to be smaller than 0.5%.

4. CONCLUSION

Putting together the results of the previous sections, we compose the final value of the in-phase force factor $\bar{f} = \bar{f}_{\text{TH}} + \bar{f}_{\text{E}} + \bar{f}_{A_{\text{E}}} + \bar{f}_{A_{\text{M}}} = 0.238 \pm 0.070$. The 0.07 error is a rather conservative value, obtained by doubling the estimated Earth albedo contribution $\bar{f}_{A_{\text{E}}}$ (see Section 2.2) plus an estimate of the thermal factor $\bar{f}_{\text{TH}}$ uncertainty. The estimate (2) of the in-phase amplitude of the synodic oscillation of the lunar orbit is then to be multiplied by a factor of $(1 + \bar{f})$, resulting in $|\delta r|_{\text{syn}} \simeq 3.65$ mm. The estimated error due to modeling limitations and/or unpredictable phenomena is about 2%, i.e., 0.08 mm, including an estimate of the contribution of the second-order coefficients $(f_{2c}, f_{2s}, f'_{2c}, f'_{2s})$ to the synodic oscillation of the lunar orbit (Nordtvedt 1995). Owing to very slow lunar rotation, no significant out-of-phase amplitude of the synodic perturbations has been found.

In this study, we focused on computing the averaged values of the functions $f(\tau)$ and $f'(\tau)$ from (3), which are needed for precise elimination of the studied effects from the LLR data on the synodic frequency, a task which is important for improving precision of the free-fall hypothesis (gravitation) test. Nordtvedt (1995) showed that analytical determination of the first-order coefficients (f_c, f_s, f'_c, f'_s) would be of interest for improving bounds on (hypothetical) gravitational "constant" time-dependence. This task remains for future work.

Finally, in the precise bounds of the contribution of the second-order coefficients $(f_{2c}, f_{2s}, f'_{2c}, f'_{2s})$ to the synodic oscillation of the lunar orbit, simply estimated in this study, rests an interesting opened problem.

ACKNOWLEDGMENTS

I thank K. Nordtvedt and X. X. Newhall for suggestions which significantly improved the original form of the manuscript. I also acknowledge

kind hospitality of OCA/CERGA (France) during summer 1996 when this work was completed.

REFERENCES

AHMAD, S. P., AND D. W. DEERING 1992. A simple analytical function for bidirectional reflectance. *J. Geophys. Res.* **97,** 18867–18886.

AFONSO, G., F. BARLIER, M. CARPINO, P. FARINELLA, F. MIGNARD, A. MILANI, AND A. M. NOBILI 1989. Orbital effects of LAGEOS seasons and eclipses. *Ann. Geophys.* **7**A, 501–514.

BURNS, J. A., P. L. LAMY, AND S. SOTER 1979. Radiation forces on small particles in the Solar System. *Icarus* **40,** 1–48.

CHANDRASEKHAR, S. 1950. *Radiative Transfer.* Clarendon, Oxford.

DAMOUR, T., AND D. VOKROUHLICKÝ 1996a. Equivalence principle and the Moon. *Phys. Rev. D* **53,** 4177–4201.

DAMOUR, T., AND D. VOKROUHLICKÝ 1996b. Testing for the preferred frame effects and the cosmic polarization using the lunar orbit. *Phys. Rev. D* **53,** 6740–6747.

DICKEY, J. O., P. L. BENDER, J. E. FALLER, X. X. NEWHALL, R. RICKLEFS, J. C. RIES, J. SHELFUS, C. VEILLET, A. WHIPPLE, J. WIANT, J. G. WILLIAMS, AND C. YODER 1994. Lunar laser ranging: A continuing legacy of the Apollo program. *Science* **265**, 482–490.

FARINELLA, P., AND D. VOKROUHLICKÝ 1996. Thermal force effects on slowly rotating, spherical artificial satellites. I. Solar heating. *Planet. Space Sci.,* **44,** 1551–1561.

FESSENKOV, V. G. 1962. Photometry of the Moon. In *Physics and Astronomy of the Moon* (Z. Kopal, Ed.), pp. 99–130. Academic Press, New York.

FOUQUART, Y., J. C. BURIEZ, M. HERMAN, AND R. S. KANDEL 1990. The influence of clouds on radiation: A climate-modeling perspective. *Rev. Geophys.* **28,** 145–166.

GLEGG, P. E., J. A. BASTIN, AND A. E. GEAR 1966. Heat transfer in lunar rock. *Mon. Not. R. Astron. Soc.* **133,** 63–66.

IRVINE, W. M. 1975. Multiple scattering in planetary atmospheres. *Icarus* **25,** 175–204.

LEBOFSKY, L. A., AND J. R. SPENCER 1989. Radiometry and thermal modeling of asteroids. In *Asteroids II* (R. Binzel, Ed.), pp. 128–147, Univ. of Arizona Press, Tucson.

LUMME, K., AND E. BOWELL 1981. Radiative transfer in the surfaces of atmosphereless bodies. I. Theory. *Astron. J.* **86,** 1694–1704.

LUMME, K., AND W. M. IRVINE 1982. Radiative transfer in the surfaces of atmosphereless bodies. III. Interpretation of lunar photometry. *Astron. J.* **87,** 1076–1082.

MIHALAS, D. 1978. *Stellar Atmospheres*. Freeman, San Francisco.

MOKHOV, I. I., AND M. E. SCHLESINGER 1994. Analysis of global cloudiness. 2. Comparison of ground-based and satellite-based cloud climatologies. *J. Geophys. Res.* **99,** 17045–17065.

MÜLLER, J., K. NORDTVEDT, AND D. VOKROUHLICKÝ 1996. Improved constraint on the α_1 PPN parameter from lunar motion. *Phys. Rev. D* **54,** 5927–5930.

NORDTVEDT, K. 1968. Equivalence principle for massive bodies. I. Phenomenology. *Phys. Rev.* **169**, 1014–1016; Equivalence principle for massive bodies. II. Theory. *Phys. Rev.* **169,** 1017–1025.

NORDTVEDT, K. 1994. Cosmic acceleration of Earth and the Moon by dark matter. *Astrophys. J.* **437,** 529–531.

NORDTVEDT, K. 1995. The relativistic orbit observables in lunar laser ranging. *Icarus* **114,** 51–62.

NORDTVEDT, K. 1996. In *Dark Matter in Cosmology, Quantum Measurements and Experimental Gravitation*, Proceedings of the XXXI Moriond Conference, in press.

NORDTVEDT, K., AND D. VOKROUHLICKÝ 1997. Recent progress in analytical modeling of the relativistic effects in the lunar motion. In *Dynamics and Astrometry of Natural and Artificial Celestial Bodies* (I. Wytrzyszczak, J.H. Lieske, and F. Mignard, Eds.), in press. Kluwer Academic, Dordrecht.

PETERSON, C. 1976. A source mechanism for meteorites controlled by the Yarkovsky effect. *Icarus* **29,** 91–111.

PETTIT, E., AND S. B. NICHOLSON 1930. Lunar radiation and temperatures. *Astrophys. J.* **71,** 102–135.

RASCHKE, E., T. H. VONDER HAAR, M. PASTERNAK, AND W. R. BANDEEN 1973. *The Radiation Balance of the Earth–Atmosphere System from Nimbus-3 Radiation Measurements.* NASA TN D-7249.

RUBINCAM, D. P. 1987. LAGEOS orbit decays due to infrared radiation from Earth. *J. Geophys. Res.* **92,** 1287–1294.

RUBINCAM, D. P. 1995. Asteroid evolution due to thermal drag. *J. Geophys. Res.* **100,** 1585–1594.

RUBINCAM, D. P., P. KNOCKE, V. R. TAYLOR, AND S. BLACKWELL 1987. Earth anisotropic reflection and the orbit of LAGEOS. *J. Geophys. Res.* **92,** 11662–11668.

SALVAIL, J. R., AND F. P. FANALE 1994. Near-surface ice on Mercury and the Moon: A topographic thermal model. *Icarus* **111,** 441–455.

SEHNAL, L. 1979. The Earth albedo model in spherical harmonics. *Bull. Astron. Inst. Czechosl.* **30,** 199–204.

SINTON , W. M. 1962. Temperatures on the lunar surface. In *Physics and Astronomy of the Moon* (Z. Kopal, Ed.), pp. 407–428. Academic Press, New York.

SPENCER, J. R., L. A. LEBOFSKY, AND M. V. SYKES 1989. Systematic biases in radiometric diameter determinations. *Icarus* **78,** 337–354.

STEPHENS, G. L., G. G. CAMPBELL, AND T. H. VONDER HAAR 1981. Earth radiation budgets. *J. Geophys. Res.* **86,** 9739–9760.

TAYLOR, V. R., AND L. L. STOWE 1984. Reflectance characteristics on uniform Earth and cloud surfaces derived from NIMBUS-7 ERB. *J. Geophys. Res.* **89,** 4987–4996.

WESSELINK, A. J. 1948. Heat conductivity and nature of the lunar surface material. *Bull. Astron. Inst. Neth.* **10,** 351–363.

WILLIAMS, J. G., X. X. NEWHALL, AND J. O. DICKEY 1996. Relativity parameters determined from lunar laser ranging. *Phys. Rev. D* **53,** 6730–6739.